

Defect bound states in the continuum of bilayer graphene without symmetry protection

Daniel Massatt,¹ Stephen P. Shipman,¹ Ilya Vekhter,² and Justin H. Wilson^{2,3}

¹*Department of Mathematics, Louisiana State University, Baton Rouge, Louisiana 70803, USA*

²*Department of Physics and Astronomy, Louisiana State University, Baton Rouge, Louisiana 70803, USA*

³*Center for Computation and Technology, Louisiana State University, Baton Rouge, Louisiana 70803, USA*

We analyze a class of bound defect states in the continuum of bilayer graphene, which emerge independent of symmetry protection or additional degrees of freedom. A comparative analysis of AA- and AB-stacked bilayer graphene demonstrates that these states originate from the intrinsic algebraic structure of the Hamiltonian rather than any underlying symmetry. This discovery provides a pathway to previously unexplored approaches in defect and band-structure engineering. We conclude with a proposed protocol for observing these states in scanning tunneling microscopy experiments.

Introduction. Defect engineering of electronic states is foundational for applications and understanding of functional materials. Modulation doping in semiconductors created field-effect transistors and enabled studies of quantum Hall states [1, 2]. Scanning tunneling spectroscopy of impurity centers is now routinely used to deduce the properties of unconventionally ordered and correlated electron systems, from superconductors to low-dimensional topological compounds [3, 4].

Strong impurity potentials can bind an electron or hole. Intuitively, if the energy of this bound state is in the energy gap of the pristine host, its wave function is localized near the impurity. In contrast, if the bound state energy is within the energy band of the host material, hybridization with the Bloch states turns this state into a resonance with a finite lifetime.

Exceptions to this picture, so-called bound states in the continuum (BIC), are well localized despite coexisting with extended states at the same energy. They have attracted considerable attention in wave mechanics and optics, since such states decouple from radiating waves, have zero leakage/linewidth, and can be used for lasing, filtering, sensing, and guiding waves [5]. Their protection is most commonly provided by symmetry constraints. In solid state systems, BICs are typically engineered via fine-tuned hopping integrals, superimposing extra degrees of freedom (*i.e.* lattice sites), or via symmetry [6–9]; we are not aware of a realistic example of a BIC that does not fall in these categories.

In this letter, we show that bilayer graphene provides such an example and investigate the behavior of the impurity states in the continuum. We contrast the localized defect states in the AA-stacked graphene, which are protected by symmetry, with the BICs in the gated AB (Bernal)-stacked graphene. In the latter case, the protection of these states against decay relies on the algebraic structure (reducibility) of the eigenvalue equation in momentum space *for fixed values of the energy*. We explicitly construct the potential yielding these states, show that (contrary to naive expectations) it can be restricted to only one pair of sites, and obtain the energies

and the wave functions of the bound state as a function of inter-bilayer coupling and gate potential. Our results lay a foundation for bulk defect engineering of the bound states in the continuum in crystalline solids.

Methodology. For a localized impurity potential \mathbf{V} , the solution in terms of Green's functions is given by the T -matrix equations $\mathbf{G} = \mathbf{G}_0 + \mathbf{G}_0 \mathbf{T} \mathbf{G}_0$ and $\mathbf{T} = (\mathbb{1} - \mathbf{V} \mathbf{G}_0)^{-1} \mathbf{V}$, where all quantities are matrices in the orbital (band) and momentum space, and $\mathbf{G}_0(E) = (E - \mathbf{H})^{-1}$ is Green's function of the pristine compound described by the Hamiltonian \mathbf{H} . The impurity states are given by the poles of the T -matrix $\det(\mathbb{1} - \mathbf{V} \mathbf{G}_0) = 0$. Generically, since $\text{Im} \mathbf{G}_0(E) \neq 0$ whenever there are band states at energy E , the pole of the T -matrix cannot occur at E , but is shifted off the real axis, indicating a finite lifetime of the impurity state. The best known exception to this rule is when the \mathbf{G}_0 and \mathbf{V} are block-diagonal, and the impurity state formed in one of the blocks does not hybridize with the extended states of other blocks due to symmetry and other constraints. We go beyond these cases and show that BIC may be enabled by specific *algebraic* structure of the Green's function.

We seek bound (exponentially decaying) solutions ψ of the eigenvalue equation

$$(E - (\mathbf{H} + \mathbf{V}))\psi = 0, \quad (1)$$

for energy E within a band of the unperturbed Hamiltonian \mathbf{H} . In scattering theory, one can view ψ as the response to a source \mathbf{J} ,

$$(E - \mathbf{H})\psi = \mathbf{J}, \quad (2)$$

with $\mathbf{J} = \mathbf{V}\psi$. In the representation used for periodic solids, the Hamiltonian and corresponding scattering matrix are functions of $z_j = \exp(i\mathbf{k} \cdot \mathbf{a}_j)$, where \mathbf{a}_j are the lattice vectors, and $\mathbf{k} = (k_1, k_2)$ is the crystal momentum. The algebraic structure that drives our analysis is natural in the complex variables $z = (z_1, z_2)$.

Central to our analysis is the eigenvalue equation, whose algebraic properties allow us to construct localized eigenstates at a given energy. Consider the dispersion function $D(z, E) = \det(E - \mathbf{H})$ whose zeroes

at real (k_1, k_2) give the electron bands $E_i(\mathbf{k})$. We will see that, for tight-binding AA- and AB-stacked graphene with nearest-neighbor hopping, $D(z, E)$ is a polynomial in a single composite variable $\eta(z)$, which is itself a polynomial in $z = (z_1, z_2)$ (with positive and negative powers). This is due to the bipartiteness of the monolayer. Factoring over η into irreducible parts $D(z, E) = D_1(z, E)D_2(z, E)$ allows us to write the solution to Eq. (2) in the form

$$\hat{\psi}(z) = \frac{\text{adj}(E - \mathbf{H}(z))\hat{\mathbf{J}}(z)}{D_1(z, E)D_2(z, E)}, \quad (3)$$

with the adjugate matrix $\text{adj}(E - \mathbf{H}(z))$, whose elements are polynomials in z . The zeroes of D_1 and D_2 provide two different components of continuous spectrum. Consider an energy E within a band associated with, say, D_2 but outside the bands associated with D_1 . For the wave function ψ to be normalizable, all roots z , with real (k_1, k_2) , of $D_2(z, E)$ must be canceled by the numerator. Since D_2 itself is irreducible, it must be cancelled identically [10]. This can be accomplished by

$$\hat{\mathbf{J}}(z) = D_2(z, E)\mathbf{p}(z), \quad (4)$$

with \mathbf{p} being any vector of polynomials. By our choice of E , $D_1(z, E) \neq 0$ for any real values of \mathbf{k} ; hence the real-space wavefunction $\psi(\mathbf{x})$ decays exponentially.

Our prescription consists of choosing a source term \mathbf{J} , determining the corresponding wave function, and then constructing from it the required impurity potential according to $\mathbf{V}\psi = \mathbf{J}$. In general, this potential is localized on as many sites as there are monomials $z_1^{n_1}z_2^{n_2}$ in D_2 . However, we show for bilayer graphene that further localization is possible. For AA stacking, this is easy, as symmetry-based decomposition makes the adjugate matrix block diagonal, and therefore the potential can be localized on one pair of aligned sites. For AB (Bernal) stacking, it is not at all obvious that the potential can be so localized. A less intuitive *algebraic and not symmetry-derived* reduction allows localization of the potential on one pair of sites. This illustrates the power of an algebraic approach. Furthermore, numerical calculations show that the state is remarkably robust, with very little spreading of the density of states as the defect potential deviates from that of the true BIC.

Monolayer graphene. The nearest-neighbor tight-binding Hamiltonian for monolayer graphene in second quantized notation is (the hopping amplitude $t = -1$)

$$H_g = \sum_{\mathbf{k}} c_{\mathbf{k}}^\dagger \mathbf{H}_s c_{\mathbf{k}}, \quad \mathbf{H}_s = \begin{bmatrix} 0 & \zeta' \\ \zeta & 0 \end{bmatrix}, \quad (5)$$

where $\zeta = 1 + z_1 + z_2$, $\zeta' = 1 + z_1^{-1} + z_2^{-1}$, and $z_j = \exp(i\mathbf{a}_j \cdot \mathbf{k})$ with lattice vectors \mathbf{a}_j shown in Fig. 1.

The dispersion function for \mathbf{H}_s ,

$$D_s(z, E) = \det(E - \mathbf{H}_s) = E^2 - \zeta\zeta' = E^2 - \eta$$

depends on the single function of the momentum [11–13]

$$\begin{aligned} \eta &\equiv \zeta\zeta' = 3 + z_1 + z_1^{-1} + z_2 + z_2^{-1} + z_1z_2^{-1} + z_2z_1^{-1} \\ &= 3 + 2\cos k_1 + 2\cos k_2 + 2\cos(k_2 - k_1). \end{aligned} \quad (6)$$

We treat η algebraically as a polynomial in the complex variables z_1 and z_2 .

Defect states in the continuum for AA stacking by symmetry. Introducing the Pauli matrices τ_i in the layer indices, the Hamiltonian for AA-stacked graphene in the basis $(1A, 1B, 2A, 2B)$ is

$$\mathbf{H}_{AA}(z) = \mathbf{1} \otimes \mathbf{H}_s + \mathbf{\Gamma} \otimes \mathbf{1} = \begin{bmatrix} \Delta & \zeta' & \gamma & 0 \\ \zeta & \Delta & 0 & \gamma \\ \gamma & 0 & -\Delta & \zeta' \\ 0 & \gamma & \zeta & -\Delta \end{bmatrix},$$

where $\mathbf{\Gamma} = \gamma\tau_1 + \Delta\tau_3$ contains the interlayer coupling γ and gating Δ . The dispersion function is

$$D(z, E) = [\zeta\zeta' - (E - \kappa)^2] [\zeta\zeta' - (E + \kappa)^2] \quad (7)$$

$= D_1(z, E)D_2(z, E)$, where $\kappa = \sqrt{\gamma^2 + \Delta^2}$. If we then implement the general procedure to find the localized state using (4), it would appear that the smallest range of the impurity potential has to be seven unit cells, since there are that many different hopping terms (monomials) in $\zeta\zeta'$, see Eq. (6). However, the symmetry of the problem allows to reduce this to a single pair of sites.

Transforming to the basis where $\mathbf{\Gamma} \propto \tau_3$ (note $\mathbf{\Gamma}$ is traceless) makes the Hamiltonian \mathbf{H}_{AA} block diagonal [14]. The eigenvalues of $\mathbf{\Gamma}$ are $\pm\kappa$ and corresponding orthonormal eigenvectors $\xi^{(1),(2)} \propto [\gamma, \pm\kappa - \Delta]^T$ determine the projectors $\mathbf{P}_\ell = |\xi^{(\ell)}\rangle\langle\xi^{(\ell)}|$. These two vectors determine two combinations of intralayer states that reduce the Hamiltonian to the orthogonal block form $\mathbf{H}_{AA} = \mathbf{P}_1 \otimes (\mathbf{H}_s + \kappa\mathbf{1}) + \mathbf{P}_2 \otimes (\mathbf{H}_s - \kappa\mathbf{1})$; this explains the shift of the spectra by κ . When $\gamma=0$, the $\xi^{(\ell)}$ yield the layer basis while for $\Delta=0$, they yield the basis of even and odd layer combinations. Block ℓ ($\ell = 1, 2$) corresponds to the $E-\mathbf{k}$ pairs that make the ℓ^{th} factor $D_\ell(z, E)$ in Eq. (7) vanish and produces the ℓ^{th} component of the spectral continuum.

Now we choose an energy within a spectral band of component 2 but within a spectral gap of component 1 and create a defect state associated with component 1. The defect must respect the block decomposition of \mathbf{H}_{AA} to ensure no broadening of the state; thus it must be of the form $\mathbf{V} = \mathbf{P}_1 \otimes V_1 + \mathbf{P}_2 \otimes V_2$, where V_1 and V_2 are local intralayer operators. Block 1 of the defective Hamiltonian is $\mathbf{P}_1 \otimes (\mathbf{H}_s + \kappa\mathbf{1} + V_1)$. The bound state is now constructed from Eqs. (2)-(3) within the subspace defined by \mathbf{P}_1 . In the equation

$$[E - (\mathbf{H}_s + \kappa)]\psi = \mathbf{J}, \quad (8)$$

let us choose $\mathbf{J} = [1, 0]^T$, meaning that the source is 1 on a selected A site, and zero on the B site in the same

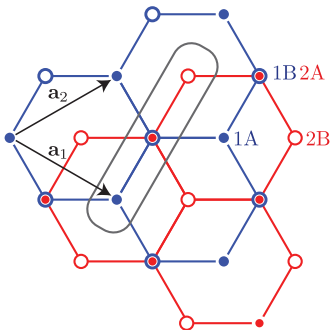


FIG. 1. Tight-binding model for AB-stacked bilayer graphene. Interlayer coupling occurs between the 1B and 2A sites only.

unit cell and zero on all other lattice sites. The condition $V_1\psi = \mathbf{J}$ is satisfied for $V_1(B) = 0$ and

$$V_1(A) = \left[\frac{E - \kappa}{(2\pi)^2} \int_0^{2\pi} \int_0^{2\pi} \frac{dk_1 dk_2}{(E - \kappa)^2 - \zeta\zeta'} \right]^{-1}. \quad (9)$$

For any γ and Δ , provided we take E in the spectral band 2 $[-\kappa, 9 - \kappa]$ but not in band 1 $[\kappa, 9 + \kappa]$, the potential V_1 creates a bound state. The relative values of the bound state on the two layers are determined by the eigenvector $\xi^{(1)}$. The value of $V_2(A)$ (with $V_2(B) = 0$) can be chosen arbitrarily, resulting in a defect of the form $\mathbf{V} = \mathbf{P}_1 \otimes V_1 + \mathbf{P}_2 \otimes V_2 = (V_1 + V_2)\mathbb{1} + (V_1 - V_2)\tau_1$ acting on one pair of aligned A sites. Hopping between the two sites vanishes when $V_1 = V_2$. On the other hand $V_1 = -V_2$ generates BIC solely by local modification the interlayer hopping amplitude.

Importantly, this method allows one to construct a set of potentials with different spatial localization that all yield BIC at the same energy. By choosing the source term to be, say, $\mathbf{J} = [1, 1]^T$ or including other nearest neighbors, one can generate defect potentials \mathbf{V} with arbitrarily small or large support range on lattice sites. Because this construction relies only on block-matrix reducibility and not on the periodicity of the Hamiltonian, it persists in the presence of a magnetic field [15].

Defect states in the continuum for AB stacking by algebraic reduction. In contrast to AA-stacking, symmetry reduction is not available for constructing bound states in the continuum for AB-stacked graphene (Fig. 1). Nevertheless, we show how the algebraic reducibility of the Fermi surface at all energies offers a mechanism to create BICs, and we demonstrate that the defect can be localized to a single 1B-2A pair.

In the same (1A, 1B, 2A, 2B) basis, the Hamiltonian and the dispersion function for Bernal stacking are

$$\mathbf{H}_{\text{AB}} = \begin{bmatrix} \Delta & \zeta' & 0 & 0 \\ \zeta & \Delta & \gamma & 0 \\ 0 & \gamma & -\Delta & \zeta' \\ 0 & 0 & \zeta & -\Delta \end{bmatrix},$$

$$D(z, E) = (\zeta\zeta')^2 - 2\zeta\zeta'(\Delta^2 + E^2) + (\Delta^2 - E^2)(\Delta^2 + \gamma^2 - E^2). \quad (10)$$

The dispersion function for *any* tight-binding Hamiltonian is a polynomial $D(z, E)$ in z and E , but the particular structure of AB-stacking causes D to be quadratic in the single composite momentum variable $\eta = \zeta\zeta'$. This allows factorization of D into a product of two factors, $D(z, E) = D_1(z, E)D_2(z, E)$, each linear in η ,

$$D_{1,2}(z, E) = \zeta\zeta' - E^2 - \Delta^2 \pm \lambda, \quad (11)$$

$$\lambda = \sqrt{4E^2\Delta^2 - \Delta^2\gamma^2 + E^2\gamma^2}.$$

Each of the factors D_ℓ contributes a set of bands to the electron dispersion as seen in Fig. 2(a). Graph-structural reasons behind this reducibility for metric-graph models are discussed in [16].

Localization of the defect. Even in the absence of factorization by symmetry, the minimal range of the impurity potential can be reduced from seven unit cells (implied by $\zeta\zeta'$, as described above) to just one pair of coupled 1B-2A sites. This can be achieved via a block decomposition $\mathbf{U}(E - \mathbf{H}_{\text{AB}})\mathbf{L} = \mathbf{\Lambda}$, where both \mathbf{U} and \mathbf{L} are polynomial in (z_1, z_2) and diagonal in the central 2×2 block with $\det \mathbf{U} = \det \mathbf{L} = 1$, and (see [14])

$$\mathbf{\Lambda} = \begin{bmatrix} 1 & 0 & 0 & 0 \\ 0 & S & 0 & 0 \\ 0 & 0 & 0 & 0 \\ 0 & 0 & 0 & 1 \end{bmatrix}. \quad (12)$$

This ensures $\det \mathbf{\Lambda} = \det S = D(z, E)$. Under this decomposition, $(E - \mathbf{H}_{\text{AB}})^{-1} = \mathbf{L}\mathbf{\Lambda}^{-1}\mathbf{U}$; so, if \mathbf{J} is nonzero only on the chosen 1B-2A sites, so also is $\mathbf{U}\mathbf{J}$. We find

$$\mathbf{L} = - \begin{bmatrix} \frac{-1}{E-\Delta} & \zeta' & 0 & 0 \\ 0 & E-\Delta & 0 & 0 \\ 0 & 0 & E+\Delta & 0 \\ 0 & 0 & \zeta & \frac{-1}{E+\Delta} \end{bmatrix},$$

$$\mathbf{U} = \begin{bmatrix} 1 & 0 & 0 & 0 \\ \frac{\zeta}{E-\Delta} & 1 & 0 & 0 \\ 0 & 0 & 1 & \frac{\zeta'}{E+\Delta} \\ 0 & 0 & 0 & 1 \end{bmatrix},$$

and $S = (\zeta\zeta' - E^2 - \Delta^2)\mathbb{1} + R$, $R = E\gamma\sigma_1 + i\Delta\gamma\sigma_2 + 2E\Delta\sigma_3$, with σ_i being the Pauli matrices in the 1B-2A space. The key observation is that the momentum dependence $\zeta\zeta'$ now appears with the identity matrix. Therefore, the eigenvalues of S as a function of $\zeta\zeta'$ are $D_{1,2}(z, E)$ and the matrix S can be diagonalized with the momentum-independent eigenvectors of R ,

$$u_1 = \begin{bmatrix} E\gamma + \Delta\gamma \\ \lambda - 2E\Delta \end{bmatrix}, \quad u_2 = \begin{bmatrix} E\gamma + \Delta\gamma \\ -\lambda - 2E\Delta \end{bmatrix},$$

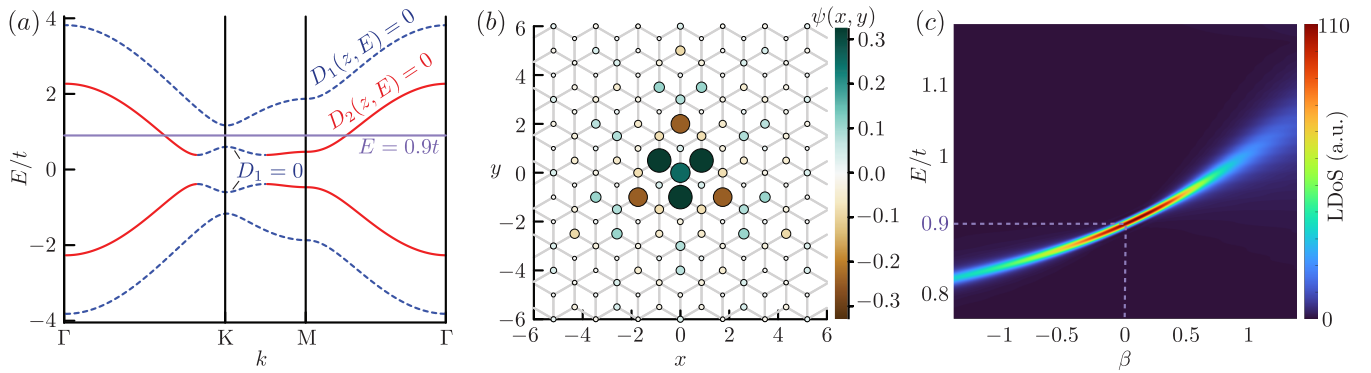


FIG. 2. Bound state in a continuum in Bernal stacked graphene. (a) Dispersion relation for AB-stacked graphene with coupling $\gamma = t$ and gating $\Delta = 0.6t$. The band in dashed blue (solid red) is associated to the factor D_1 (D_2). The horizontal line indicates an energy within a D_2 -band and a D_1 -gap for which a bound defect state exists. (b) The bound state ψ created by a defect potential localized at a single 1B-2A pair of orbitals; on the 1B-2A sites, the 1B value of ψ is shown. (c) The local density of states (LDoS) is peaked at the point of the embedded state indicated by the dotted lines. Perturbation by $\approx \beta[t, 0.78t]$ of the potential on the 1B-2A sites causes only weak spreading of the LDoS, illustrating the robustness of the embedded state. The LDoS is computed using the kernel polynomial method (KPM) [17].

ensuring locality of the source term on a single pair of sites. Without gating, the eigenvectors reduce to the even and odd combinations of the sites, $u_1 = [1, 1]^t$ and $u_2 = [1, -1]^t$.

To construct a BIC, let E be an energy in a D_2 -band but not in a D_1 -band, and set $\hat{\mathbf{J}}(z) = \mathcal{N}u_1$ in Eq. (2) (\mathcal{N} is a normalization constant). The response is $\hat{\psi}(z) = (E - \mathbf{H}_{\text{AB}})^{-1}\hat{\mathbf{J}}(z)$, or

$$\hat{\psi}(z) = \frac{-\mathcal{N}}{D_1(z, E)} \begin{bmatrix} (E\gamma + \Delta\gamma)\zeta' \\ (E\gamma + \Delta\gamma)(E - \Delta) \\ (\lambda - 2E\Delta)(E + \Delta) \\ (\lambda - 2E\Delta)\zeta \end{bmatrix}.$$

Fourier transforming ψ to solve $\mathbf{V}\psi = \mathbf{J}$ we obtain

$$\begin{aligned} V(1B) &= [(E - \Delta)F(E, \gamma, \Delta)]^{-1} \\ V(2A) &= [(E + \Delta)F(E, \gamma, \Delta)]^{-1} \end{aligned} \quad (13)$$

with

$$F(E, \gamma, \Delta) = - \int_0^{2\pi} \int_0^{2\pi} \frac{d^2k}{(2\pi)^2} [D_1(e^{ik_1}, e^{ik_2}, E)]^{-1}.$$

This provides a prescription for constructing a localized state at a desired energy E for a given gating. A computation of a localized state is shown in Fig. 2(b,c). The required values of the potential depending on the gating and the energy of the BIC are given in Fig. 3.

Robustness to perturbations. It is natural to ask how sensitive the bound state is to deviations of the potential from the values given in Eq. (13). Numerical evaluation of the local density of states in Fig. 2(c) shows that these bound states in the continuum are remarkably robust to perturbations of the defect potential, despite the lack of symmetry protection.

General structure. Our work provides a pathway to generating embedded states. For a lattice with a basis (in layer and/or site space) the tight-binding Hamiltonian is a matrix whose entries are the Laurent polynomials (allowing negative powers) in $z_j = \exp(i\mathbf{a}_j \cdot \mathbf{k})$ with $j = 1, \dots, d$ in dimension d . We require $\mathbf{U}(E - \mathbf{H})\mathbf{L} = \mathbf{\Lambda}$, where $\mathbf{\Lambda} = \sum_{\ell} D_{\ell}(z, E)\mathbf{P}_{\ell} + \mathbf{Q}$ for complementary projectors \mathbf{P}_{ℓ} and \mathbf{Q} such that $\sum_{\ell} \mathbf{P}_{\ell} + \mathbf{Q} = \mathbf{1}$, $D_{\ell}(z, E)$ are polynomials of z_j , and $\mathbf{U}, \mathbf{L} \in \text{SL}(N, \mathbb{C}[z_j, z_j^{-1}])$, which means they are polynomial in z_j with determinant equal to 1. This is precisely the conditions we imposed above.

In this case the above procedure can be used to engineer a *local* source term \mathbf{J} such that $\mathbf{U}\hat{\mathbf{J}}$ only has support in the subspace of the projector \mathbf{P}_{ℓ} . Then $\hat{\psi} = D_{\ell}^{-1}(z, E)\mathbf{L}\mathbf{U}\hat{\mathbf{J}}$, is the bound state, and the condition $\mathbf{J} = \mathbf{V}\psi$ determines a local V that generates ψ as an eigenstate at that energy. While at present we are not aware of a universal procedure for finding the Hamiltonians that are factorizable in this manner, our example of Bernal stacked graphene strongly indicates that such models are relatively common and deserve future studies.

Conclusion. Using a nearest-neighbor tight-binding model, we have demonstrated that Bernal-stacked graphene admits exponentially localized (bound) defect states at energies embedded within a spectral band. To our knowledge, this is the first example of bound states in the continuum that are induced not by symmetries, but by the algebraic reducibility (polynomial factorization) of the dispersion function. Generically for tight-binding models, the spatial extent of the defect increases with the polynomial complexity of the irreducible factor corresponding to the spectral band in which the bound state energy lies. Remarkably however, we showed

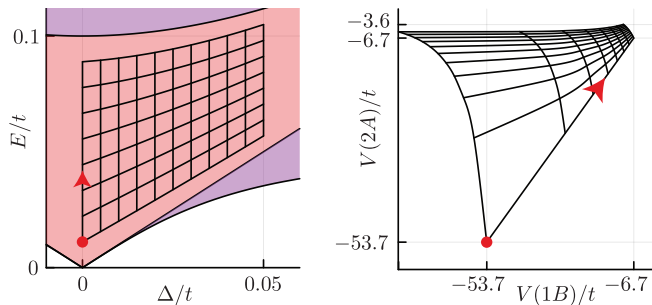


FIG. 3. The potential required to create a defect state at an energy and gating. We plot the mapping from (E, Δ) (left) to $(V(1B), V(2A))$ (right) as defined by Eq. (13) with $\gamma = 0.1t$. The red circle and arrow on both map to one another. In the E vs. Δ plot, white space represents a gap, purple represents both D_1 - and D_2 -bands at that energy, and light red represents the presence of a D_2 -band and D_1 -gap.

that Bernal-stacked graphene exhibits additional algebraic structure that allows localization of the defect to just one pair of 1B-2A orbitals.

The BIC should be observable in the local density of states (LDoS) measured by local tunneling probes. Our proposal is to (1) Induce a defect potential at an AB-stacked site either via impurity or tip, (2) vary the energy to map out the broad resonant feature in the LDoS, and (3) vary the gating to match the conditions in Eq. (13). The broad resonant feature should narrow in energy and achieve a minimum where the condition for a BIC is met, similarly to what is seen in Fig. 2(c).

There is a general multi-terminal theory describing resonances and BICs in tight-binding models [18] without specific reference to any particular structure. It remains for now an open question whether the structure we present for Bernal-stacked graphene fits into this formalism. In contrast, our approach yields a prescription for generating BICs, and as such should be applicable to a wide range of point and line defects in layered compounds, topological materials such as higher-order topological insulators, and other systems of current interest [19, 20]. We anticipate that these defect states could be arranged in a larger super-structure to build flat bands within bands.

Acknowledgements. This material is based upon work supported by the National Science Foundation under Grant No. DMS-2206037. J.H.W. acknowledges support from NSF CAREER Grant No. DMR-2238895. I. V. and J. H. W. were supported in part by grant NSF PHY-2309135 to the Kavli Institute for Theoretical Physics.

- [2] B. I. Halperin and J. K. Jain, eds., *Fractional Quantum Hall Effects: New Developments* (World Scientific, New Jersey, 2020).
- [3] Ø. Fischer, M. Kugler, I. Maggio-Aprile, C. Berthod, and C. Renner, Scanning tunneling spectroscopy of high-temperature superconductors, *Reviews of Modern Physics* **79**, 353 (2007).
- [4] J.-X. Yin, S. H. Pan, and M. Zahid Hasan, Probing topological quantum matter with scanning tunnelling microscopy, *Nature Reviews Physics* **3**, 249 (2021).
- [5] C. W. Hsu, B. Zhen, A. D. Stone, J. D. Joannopoulos, and M. Soljačić, Bound states in the continuum, *Nature Reviews Materials* **1**, 16048 (2016).
- [6] J. W. González, M. Pacheco, L. Rosales, and P. A. Orellana, Bound states in the continuum in graphene quantum dot structures, *EPL (Europhysics Letters)* **91**, 66001 (2010).
- [7] M. I. Molina, A. E. Miroschnichenko, and Y. S. Kivshar, Surface bound states in the continuum, *Phys. Rev. Lett.* **108**, 070401 (2012).
- [8] G. Corrielli, G. Della Valle, A. Crespi, R. Osellame, and S. Longhi, Observation of surface states with algebraic localization, *Phys. Rev. Lett.* **111**, 220403 (2013).
- [9] N. Cortés, L. Chico, M. Pacheco, L. Rosales, and P. A. Orellana, Bound states in the continuum: Localization of Dirac-like fermions, *EPL (Europhysics Letters)* **108**, 46008 (2014).
- [10] P. Kuchment and B. Vainberg, On the structure of eigenfunctions corresponding to embedded eigenvalues of locally perturbed periodic graph operators, *Comm. Math. Phys.* **268**, 673 (2006).
- [11] A. H. Castro Neto, F. Guinea, N. M. R. Peres, K. S. Novoselov, and A. K. Geim, The electronic properties of graphene, *Rev. Mod. Phys.* **81**, 109 (2009).
- [12] E. McCann and M. Koshino, The electronic properties of bilayer graphene, *Reports on Progress in Physics* **76**, 056503 (2013).
- [13] P. Kuchment and O. Post, On the spectra of carbon nanostructures, *Comm. Math. Phys.* **275**, 805 (2007).
- [14] See Supplemental Material at [URL will be inserted by publisher] for calculational details.
- [15] S. P. Shipman and J. Villalobos, Stable defect states in the continuous spectrum of bilayer graphene with magnetic field, *Physica D: Nonlinear Phenomena* **455**, 133891 (2023).
- [16] L. Fisher, W. Li, and S. P. Shipman, Reducible Fermi surface for multi-layer quantum graphs including stacked graphene, *Comm. Math. Phys.* **385**, 1499 (2021).
- [17] A. Weiße, G. Wellein, A. Alvermann, and H. Fehske, The kernel polynomial method, *Rev. Mod. Phys.* **78**, 275 (2006).
- [18] A. A. Gorbatsevich and N. M. Shubin, Unified theory of resonances and bound states in the continuum in Hermitian tight-binding models, *Physical Review B* **96**, 205441 (2017).
- [19] M. Takeichi and S. Murakami, Topological linelike bound states in the continuum, *Physical Review B* **99**, 035128 (2019).
- [20] A. Cerjan, M. Jürgensen, W. A. Benalcazar, S. Mukherjee, and M. C. Rechtsman, Observation of a Higher-Order Topological Bound State in the Continuum, *Physical Review Letters* **125**, 213901 (2020).

[1] R. E. Prange and S. M. Girvin, eds., *The Quantum Hall Effect*, 2nd ed., Graduate Texts in Contemporary Physics (Springer-Verlag, New York, 1990).

Supplementary material for Defect bound states in the continuum of bilayer graphene without symmetry protection

Daniel Massatt*, Stephen P. Shipman*, Ilya Vekhter†, Justin Wilson†

*Department of Mathematics and †Department of Physics, Louisiana State University

The mono-layer tight-binding Hamiltonian acts in the Hilbert space $\mathcal{H} = \ell^2(\mathbb{Z}^2, \mathbb{C}^2)$. For a wave function $\psi \in \mathcal{H}$ and $(n_1, n_2) \in \mathbb{Z}^2$, $\psi(n_1, n_2)$ has two components: $\psi_1(n_1, n_2)$ is the value at the A site shifted by $n_1\mathbf{a}_1 + n_2\mathbf{a}_2$ and $\psi_2(n_1, n_2)$ is the value at the shifted B site. The Pauli matrices are

$$\tau_1 = \begin{bmatrix} 0 & 1 \\ 1 & 0 \end{bmatrix}, \quad \tau_2 = \begin{bmatrix} 0 & -i \\ i & 0 \end{bmatrix}, \quad \tau_3 = \begin{bmatrix} 1 & 0 \\ 0 & -1 \end{bmatrix}.$$

AA stacking. The Hamiltonian for AA-stacked graphene is $\mathbf{H}_{AA} = \mathbb{1} \otimes \mathbf{H}_s + \mathbf{\Gamma} \otimes \mathbb{1}$. Let $\mathbf{P}_j = |\xi^{(j)}\rangle\langle\xi^{(j)}|$ be the projections onto the eigenspaces of $\mathbf{\Gamma}$. The Hamiltonian for AA-stacked graphene with a local defect can be written as $\mathbf{H}_{AA} + \mathbf{V}$, where \mathbf{V} is a defect operator that commutes with $\mathbf{\Gamma}$ so that it is simultaneously block diagonalized with the periodic bulk,

$$\begin{aligned} \mathbf{H}_{AA} &= \mathbf{P}_1 \otimes (\mathbf{H}_s + \kappa\mathbb{1}) + \mathbf{P}_2 \otimes (\mathbf{H}_s - \kappa\mathbb{1}) \quad (1) \\ \mathbf{V} &= \mathbf{P}_1 \otimes V_1\mathbf{P}_A + \mathbf{P}_2 \otimes V_2\mathbf{P}_A. \quad (2) \end{aligned}$$

\mathbf{P}_A is the projection onto one A site of the single-layer graphene lattice, under the assumption that \mathbf{V} is localized at one pair of aligned A sites.

Assuming that an energy E lies in the continuum for the \mathbf{P}_2 component, we consider the forced system

$$(E - (\mathbf{H}_s + \kappa\mathbb{1} + V_1\mathbf{P}_A))\psi = \mathbf{J}. \quad (3)$$

Putting $\mathbf{J} = [1, 0]$ is the simplest case; this means that $\mathbf{J}(A) = 1$ and $\mathbf{J}(B) = 0$, where A and B are sites in a reference (unshifted) period of the pristine graphene structure, and that \mathbf{J} is zero on all other sites. In matrix form in momentum space, this is

$$\begin{bmatrix} E - \kappa & -\zeta' \\ -\zeta & E - \kappa \end{bmatrix} \begin{bmatrix} \hat{\psi}_1(z) \\ \hat{\psi}_2(z) \end{bmatrix} = \begin{bmatrix} 1 \\ 0 \end{bmatrix},$$

with solution at the reference A site equal to $\psi(A) = \psi_1(0, 0)$ (that is, at $n_1 = 0$ and $n_2 = 0$),

$$\psi(A) = \frac{E - \kappa}{(2\pi)^2} \int_0^{2\pi} \int_0^{2\pi} \frac{dk_1 dk_2}{(\kappa - E)^2 - \zeta\zeta'}.$$

We then enforce $V_1\psi_1(A) = \mathbf{J}(A) = 1$, which yields

$$V_1 = \left[\frac{E - \kappa}{(2\pi)^2} \int_0^{2\pi} \int_0^{2\pi} \frac{dk_1 dk_2}{(\kappa - E)^2 - \zeta\zeta'} \right]^{-1}.$$

AB stacking. The determinant of $E - \mathbf{H}_{AB}$ is computed as follows. Write the matrix in block form $E - \mathbf{H}_{AB} = \begin{bmatrix} A & B \\ B^* & C \end{bmatrix}$ and use the formula

$$\det(E - \mathbf{H}_{AB}) = |A| |C - B^*A^{-1}B|,$$

in which $|\cdot|$ indicates the determinant. A simple computation yields

$$B^*A^{-1}B = \gamma^2 \begin{bmatrix} (A^{-1})_{22} & 0 \\ 0 & 0 \end{bmatrix}.$$

Bilinearity of the determinant then gives

$$|C - B^*A^{-1}B| = |C| - \gamma^2 (A^{-1})_{22} C_{22}.$$

The determinants of A and C are

$$|A| = (\Delta - E)^2 - \zeta\zeta', \quad |C| = (\Delta + E)^2 - \zeta\zeta',$$

and one computes that

$$(A^{-1})_{22} = \frac{E - \Delta}{|A|}, \quad C_{22} = \Delta + E.$$

Putting these results together yields

$$\begin{aligned} \det(E - \mathbf{H}_{AB}) &= |A| \left[|C| + \gamma^2 \frac{\Delta^2 - E^2}{|A|} \right] \\ &= |A| |C| + \gamma^2 (\Delta^2 - E^2) \\ &= (\zeta\zeta')^2 - 2(\Delta^2 + E^2)\zeta\zeta' + (\Delta^2 - E^2)(\Delta^2 + \gamma^2 - E^2) \\ &= D(z, E). \end{aligned}$$

The computation of $\mathbf{U}(E - \mathbf{H}_{AB})\mathbf{L} = \mathbf{\Lambda}$ is mundane: First, $\mathbf{U}(E - \mathbf{H}_{AB}) =$

$$= - \begin{bmatrix} \Delta - E & \zeta' & 0 & 0 \\ 0 & \frac{\zeta\zeta' - (E - \Delta)^2}{E - \Delta} & \gamma & 0 \\ 0 & \gamma & \frac{\zeta\zeta' - (E + \Delta)^2}{E + \Delta} & 0 \\ 0 & 0 & \zeta & -(E + \Delta) \end{bmatrix};$$

then, $\mathbf{U}(E - \mathbf{H}_{AB})\mathbf{L} =$

$$= \begin{bmatrix} 1 & 0 & 0 & 0 \\ 0 & \zeta\zeta' - (E - \Delta)^2 & \gamma(E + \Delta) & 0 \\ 0 & \gamma(E - \Delta) & \zeta\zeta' - (E + \Delta)^2 & 0 \\ 0 & 0 & 0 & 1 \end{bmatrix}.$$

The 2×2 matrix in the middle concerns the 1B and 2A sites,

$$S = (\zeta\zeta' - E^2 - \Delta^2)I_2 + \begin{bmatrix} 2E\Delta & \gamma(E + \Delta) \\ \gamma(E - \Delta) & -2E\Delta \end{bmatrix},$$

wherein the last matrix is

$$R = E\gamma\sigma_1 + i\Delta\gamma\sigma_2 + 2E\Delta\sigma_3.$$

Using the anticommutating property $\sigma_i\sigma_j + \sigma_j\sigma_i = 0$ for $i \neq j$, one obtains

$$\begin{aligned} (aI + b\sigma_1 + c\sigma_2 + d\sigma_3)(aI - b\sigma_1 - c\sigma_2 - d\sigma_3) \\ = (a^2 - (b^2 + c^2 + d^2))I. \end{aligned}$$

Since $b\sigma_1 + c\sigma_2 + d\sigma_3$ is trace-free and its determinant is $-b^2 - c^2 - d^2$, its eigenvalues are $\lambda = \pm\sqrt{b^2 + c^2 + d^2}$, with eigenvectors $[b - ic, \pm\lambda - d]^t$.

Applying all this to $S = \zeta\zeta' - E^2 - \Delta^2 + R$ yields

$$((\zeta\zeta' - E^2 - \Delta^2)I + R)((\zeta\zeta' - E^2 - \Delta^2)I - R) = D(z, E)I$$

so that

$$S^{-1} = \frac{(\zeta\zeta' - E^2 - \Delta^2)I - R}{D(z, E)}$$

and the eigenvalues of R are

$$\lambda = \pm\sqrt{E^2\gamma^2 - \Delta^2\gamma^2 + 4E^2\Delta^2},$$

with corresponding eigenvectors

$$u_{1,2} = \begin{bmatrix} E\gamma + \Delta\gamma \\ \pm\lambda - 2E\Delta \end{bmatrix}$$

in which u_1 is for eigenvalue λ and u_2 for eigenvalue $-\lambda$.

Now consider the equation $(E - \mathbf{H}_{AB})\psi = \mathbf{J}$ with the source \mathbf{J} localized at the coupled 1B-2A sites equal to u_1 and zero elsewhere. In the momentum variable, this is

$$\hat{\mathbf{J}}(z) = \begin{bmatrix} 0 \\ E\gamma + \Delta\gamma \\ \lambda - 2E\Delta \\ 0 \end{bmatrix}. \quad (4)$$

Using $(E - \mathbf{H}_{AB})^{-1} = \mathbf{L}\Lambda^{-1}\mathbf{U}$, one computes the response in momentum space,

$$\begin{aligned} \hat{\psi}(z) &= (E - \hat{\mathbf{H}}_{AB})^{-1} \hat{\mathbf{J}}(z) \\ &= \frac{-1}{D_1(z, E)} \begin{bmatrix} (E\gamma + \Delta\gamma)\zeta' \\ (E\gamma + \Delta\gamma)(E - \Delta) \\ (\lambda - 2E\Delta)(E + \Delta) \\ (\lambda - 2E\Delta)\zeta \end{bmatrix}. \end{aligned}$$

Fourier inversion yields the wavefunction in space. On the 1B site of the reference (unshifted) period, one obtains

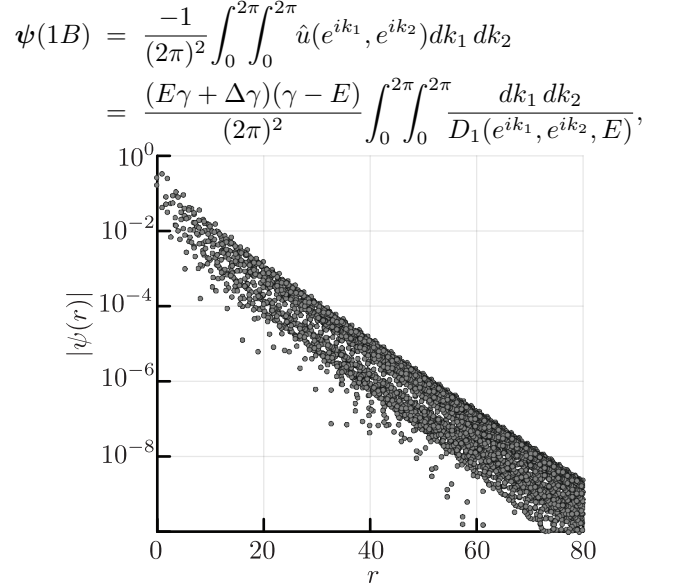


FIG. 1. The exponential localization of the embedded state with $r = \sqrt{x^2 + y^2}$ from the state shown in Fig. 2 of the main text. The potential that achieves this state is $V(1B) \approx -4.14t$ and $V(2A) \approx -0.83t$.

and on the 2A site, one obtains

$$\begin{aligned} \psi(2A) &= \frac{-1}{(2\pi)^2} \int_0^{2\pi} \int_0^{2\pi} \hat{u}(e^{ik_1}, e^{ik_2}) dk_1 dk_2 \\ &= \frac{(2E\Delta - \lambda)(E + \Delta)}{(2\pi)^2} \int_0^{2\pi} \int_0^{2\pi} \frac{dk_1 dk_2}{D_1(e^{ik_1}, e^{ik_2}, E)}. \end{aligned}$$

Now enforcing the condition $\mathbf{V}\psi = \mathbf{J}$ and assuming \mathbf{V} consists only of on-site potentials yields

$$\begin{aligned} V(1B)\psi(1B) &= \mathbf{J}(1B) = E\gamma + \Delta\gamma \\ V(2A)\psi(2A) &= \mathbf{J}(2A) = \lambda - 2E\Delta \end{aligned} \quad (5)$$

and ultimately

$$\begin{aligned} V(1B) &= - \left[\frac{E - \Delta}{(2\pi)^2} \int_0^{2\pi} \int_0^{2\pi} \frac{dk_1 dk_2}{D_1(e^{ik_1}, e^{ik_2}, E)} \right]^{-1}, \\ V(2A) &= - \left[\frac{E + \Delta}{(2\pi)^2} \int_0^{2\pi} \int_0^{2\pi} \frac{dk_1 dk_2}{D_1(e^{ik_1}, e^{ik_2}, E)} \right]^{-1}. \end{aligned} \quad (6)$$

Figure 2 shows the broadening of the embedded state under random disorder. Figure 1 verifies the exponential localization of the embedded states.

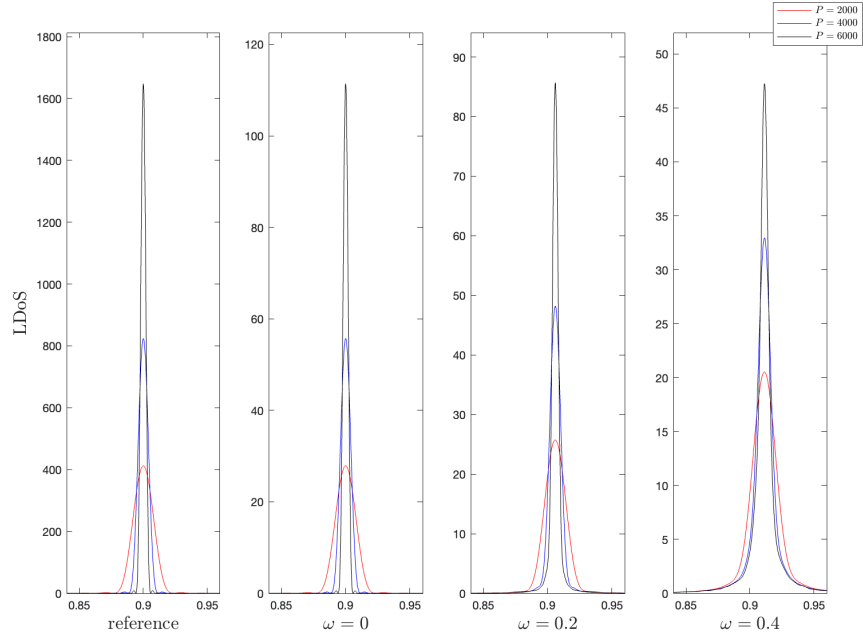


FIG. 2. Potential V is chosen such that $\mathbf{H}_{AB} + V$ admits an embedded state at $E = .9t$. V_ω is a random potential composed of on-site i.i.d. entries taking values between $[-\omega t, \omega t]$. LDoS taken at the V_{1B} site is plotted centered at $E = 0.9t$ for three different values of ω for three orders of Chebyshev polynomial approximations of the Gaussian. We plot the reference Chebyshev approximation of a Gaussian on the far-left. It can be seen for $\omega = 0$ there is a perfect embedded state, while for $\omega \neq 0$ the state exhibits spectral broadening.